Metabolic Engineering Communications 20 (2025) e00260

Contents lists available at ScienceDirect

Metabolic Engineering Communications

journal homepage: www.elsevier.com/locate/mec

^{13}C-metabolic flux analysis of *Saccharomyces cerevisiae* in complex media

Hayato Fujiwara [a], Nobuyuki Okahashi [a,b,c], Taisuke Seike [a], Fumio Matsuda [a,b,c,*]

[a] Department of Bioinformatic Engineering, Graduate School of Information Science and Technology, Osaka University, 1-5 Yamadaoka, Suita, Osaka, 565-0871, Japan
[b] Osaka University Shimadzu Omics Innovation Research Laboratories, Osaka University, 2-1 Yamadaoka, Suita, Osaka, 565-0871, Japan
[c] Industrial Biotechnology Initiative Division, Institute for Open and Transdisciplinary Research Initiatives, Osaka University, 2-1 Yamadaoka, Suita, Osaka, 565-0871, Japan

ARTICLE INFO

Handling Editor: Mattheos Koffas

Keywords:
^{13}C-based metabolic flux analysis
Central carbon metabolism
Saccharomyces cerevisiae
Complex media

ABSTRACT

Saccharomyces cerevisiae is often cultivated in complex media for applications in food and other biochemical production. However, ^{13}C-metabolic flux analysis (^{13}C-MFA) has been conducted for *S. cerevisiae* cultivated in synthetic media, resulting in a limited understanding of the metabolic flux distributions under the complex media. In this study, ^{13}C-MFA was applied to *S. cerevisiae* cultivated in complex media to quantify the metabolic fluxes in the central metabolic network. *S. cerevisiae* was cultivated in a synthetic dextrose (SD) medium supplemented with 20 amino acids (SD + AA) and yeast extract peptone dextrose (YPD) medium. The results revealed that glutamic acid, glutamine, aspartic acid, and asparagine are incorporated into the TCA cycle as carbon sources in parallel with glucose consumption. Based on these findings, we successfully conducted ^{13}C-MFA of *S. cerevisiae* cultivated in SD + AA and YPD media using parallel labeling and measured amino acid uptake rates. Furthermore, we applied the developed approach to ^{13}C-MFA of yeast cultivated in malt extract medium. The analysis revealed that the metabolic flux through the anaplerotic and oxidative pentose phosphate pathways was lower in complex media than in synthetic media. Owing to the reduced carbon loss by the branching pathways, carbon flow toward ethanol production via glycolysis could be elevated. ^{13}C-MFA of *S. cerevisiae* cultured in complex media provides valuable insights for metabolic engineering and process optimization in industrial yeast fermentation.

1. Introduction

Saccharomyces cerevisiae has been used extensively as a model organism to investigate biological systems, including metabolism (Boone, 2014; Hackett et al., 2016; Mustacchi et al., 2006; Nielsen, 2019). Metabolic analysis studies have predominantly employed synthetic media such as synthetic dextrose (SD) because of their high reproducibility, compatibility with auxotrophic markers, and minimal interference from medium components during metabolome analyses (Kim and Kim, 2017). Additionally,^{13}C-metabolic flux analysis (^{13}C-MFA) has been applied to *S. cerevisiae* to quantify metabolic fluxes in the central metabolic network (Blank et al., 2005; Christen and Sauer, 2011; Frick and Wittmann, 2005; Wasylenko and Stephanopoulos, 2015; Yatabe et al., 2021; Yuzawa et al., 2021). ^{13}C-MFA has been an important tool in metabolic engineering and process optimization (Wiechert, 2001). ^{13}C-MFA helps identify which pathways to upregulate or downregulate by comparison between an optimal flux distribution for target production and a measured flux distribution determined by ^{13}C-MFA (Costenoble et al., 2007; Frick and Wittmann, 2005; Ghosh et al., 2016; Hayakawa et al., 2015; Pitkanen et al., 2003; Sonderegger et al., 2004). ^{13}C-MFA also reveals the metabolic state of *S. cerevisiae* cells under various cultivation conditions (Hayakawa et al., 2018; Kajihata et al., 2015). However, ^{13}C-MFA is conducted using a synthetic medium because all the carbon sources must be accounted for when tracing ^{13}C labels from a carbon source to the intracellular metabolites (Antoniewicz, 2015; Wiechert, 2001; Zamboni et al., 2009).

Abbreviations: **G6P**, glucose-6-phosphate; **F6P**, fructose-6-phosphate; **FBP**, fructose-1,6-bisphosphate; **DHAP**, dihydroxyacetone phosphate; **GAP**, glyceraldehyde-3-phosphate; **Pyr$_{cyt}$**, cytosolic pyruvate; **Pyr$_{mit}$**, mitochondrial pyruvate; **AcCOA$_{cyt}$**, cytosolic acetyl-CoA; **AcCOA$_{mit}$**, mitochondrial acetyl-CoA; **AcAl**, acetaldehyde; **IsoCit**, isocitrate; **aKG**, α-ketoglutarate; **Suc**, succinate; **Mal**, malate; **OAA$_{cyt}$**, cytosolic oxaloacetate; **OAA$_{mit}$**, mitochondrial 0xaloacetate; **Ru5P**, ribulose-5-phosphate; **R5P**, ribose-5-phosphate; **Xu5P**, xylulose-5-phosphate; **S7P**, sedoheptulose-7-phosphate; **E4P**, erythrose-4-phosphate.

* Corresponding author. Department of Bioinformatic Engineering, Graduate School of Information Science and Technology, Osaka University, 1-5 Yamadaoka, Suita, Osaka 565-0871, Japan.
E-mail address: fmatsuda@ist.osaka-u.ac.jp (F. Matsuda).

https://doi.org/10.1016/j.mec.2025.e00260
Received 16 August 2024; Received in revised form 24 February 2025; Accepted 31 March 2025
Available online 1 April 2025

S. cerevisiae serves as a host for metabolic engineering applications and is widely used in the food industry for baking and brewing processes (Borodina and Nielsen, 2014; Legras et al., 2007; Lian et al., 2018; Volk et al., 2023). Complex media containing yeast extract, molasses, and malt extracts are typically used for brewing and for the production of baker's yeast and biochemicals. This is because the availability of building blocks such as amino acids, nucleic acids, and lipids in these media alleviates the burden of *de novo* biosynthesis, potentially leading to improved growth rates and enhanced conversion of sugars into desired products such as ethanol (Eliodorio et al., 2023; Hahn-Hagerdal et al., 2005). Faster growth in complex media has been also achieved through proteomic reallocation from amino acid biosynthesis to ribosomes (Bjorkeroth et al., 2020).

Another potential advantage of complex media is the possibility of utilizing amino acids as supplementary carbon sources. Budding yeast contains genes encoding enzymes responsible for the degradation of various amino acids into pyruvate or acetyl-CoA (Forster et al., 2003; Nookaew et al., 2011). However, the extent to which amino acids act as carbon sources in parallel to glucose catabolism remains poorly understood. Consequently, ^{13}C-MFA has not been extensively applied to *S. cerevisiae* cultivated in complex media, resulting in a limited understanding of the metabolic flux distributions under these conditions (Stewart et al., 2010).

Recently, ^{13}C-MFA in complex media has provided a better understanding of industrial cell factories (Schwechheimer et al., 2018c). For example, ^{13}C-MFA of *Ashbya gossypii* producing riboflavin was conducted under complex nutrient conditions by four parallel ^{13}C-labeled tracer studies using [U-$^{13}C_2$]glycine, [^{13}C]formate, [U-$^{13}C_5$]glutamate, and [U-^{13}C]yeast extract combined with gas chromatography (GC)-mass spectrometry (MS), liquid chromatography (LC)-MS, and one- and two-dimensional nuclear magnetic resonance measurements (Schwechheimer et al., 2018a, 2018b). The metabolic flux distribution of lactic acid bacteria under simulated cocoa pulp fermentation conditions was estimated using a parallel-labeling experiment (Adler et al., 2013). ^{13}C-MFA of antibody-producing Chinese hamster ovary cells was also achieved by measuring amino acid uptake rates and performing a labeling experiment using a 50:50 mixture of [1,2–$^{13}C_2$]glucose and [U-$^{13}C_6$]glucose (Templeton et al., 2017). These trials indicated that parallel labeling and measurement of amino acid uptake rates were required for ^{13}C-MFA in complex media.

In this study, we extended the application of ^{13}C-MFA to *S. cerevisiae* cultivated in a complex medium. Initially, batch cultures were performed in SD medium supplemented with 20 amino acids (SD + AA) and yeast extract peptone dextrose (YPD) medium to determine the amino acids that contribute to central carbon metabolism in parallel with glucose catabolism. The results revealed that glutamic acid, glutamine, aspartic acid, and asparagine were incorporated into the TCA cycle as carbon sources, in parallel with glucose consumption. Based on these findings, we successfully conducted ^{13}C-MFA on cells cultivated in SD + AA, YPD, and malt extract media using parallel labeling and measured amino acid uptake rates. ^{13}C-MFA revealed that the metabolic flux through the anaplerotic and oxidative pentose phosphate pathways was lower in complex media than in synthetic media.

2. Materials and methods

2.1. Yeast strain and cultivation method

A diploid of S288C, BY4947 (X2180-1A × X2180-1B), was obtained from the National Bio-Resource Project (https://yeast.nig.ac.jp/yeast/top.xhtml). All chemicals and reagents were purchased from FUJIFILM Wako Pure Chemical Co. (Osaka, Japan), unless otherwise specified. All cultures were pre-cultured on a test tube scale using YPD medium (1 % Bacto yeast extract (Becton Dickinson), 2 % Bacto peptone (Becton Dickinson), and 2 % glucose). A single colony of BY4947 cells was inoculated into 5 mL of medium and cultured overnight at 30 °C, 150 rpm. SD, SD + AA, YPD, and malt extract (ME) media were used for the pre-culture and main cultures. SD medium consisted of 0.5 % glucose and 0.67 % Difco yeast nitrogen base without amino acids (Becton Dickinson). The SD + AA medium was prepared by supplementing the SD medium with each of the following amino acids at a concentration of 1 mM: Asp, Glu, Asn, Ser, Gln, His, Gly, Arg, Ala, Pro, Val, Met, Ile, Leu, Phe, Trp, Lys, Thr, Tyr, and Cys 2HCl. ME medium consisted of 0.6 % glucose and 0.6 % malt extract (Nacalai Tesque, Kyoto, Japan). The final glucose concentration of ME was 43.5 ± 0.33 mM by HPLC analysis. For ^{13}C-MFA, glucose in the main culture was replaced with [1–^{13}C]glucose or [U-^{13}C]glucose (Cambridge Isotope Laboratories, Tewksbury, MA, USA; >99 % purity). The ratio of unlabeled glucose in ME was 25 %. Pre-cultures and main cultures were carried out in 200 mL baffled flasks, and yeast was inoculated into 50 mL of the medium at an initial OD_{600} of 0.05 and cultured at 30 °C, 150 rpm using a shaker (G BR-200, TAITEC, Tokyo, Japan).

2.2. Measurement of culture profiles

The cell concentration was measured as turbidity at a wavelength of 600 nm (optical density, OD_{600}) using a UV–visible spectrophotometer (UV-1280, Shimadzu, Kyoto, Japan). The cell dry mass was determined after centrifugation and drying the cells at 60 °C until a constant weight was achieved. A high-performance liquid chromatograph (HPLC Prominence, Shimadzu) equipped with a refractive index detector (RI) was used to measure the glucose, fructose, ethanol, acetic acid, and glycerol concentrations, following a previously described method (Taniguchi et al., 2024). The amino acid concentrations in the medium were measured using the AccQ tag method (Waters, Milford, MA, USA). First, 60 μL of AccQ•Tag ultra Borate Buffer and 10 μL of 1 mM 4-amino-3-hydroxybutyric acid as an internal standard were added to 10 μL of filter-sterilized medium and mixed by vortexing. Next, 20 μL of AccQ•Tag ultra reagent was added, vortexed for 10 s, and heated at 55 °C for 10 min in a DeepWell Maximizer (M BR-022UP, TAITEC). The mixture (80 μL) was used for the HPLC analysis (Prominence, Shimadzu) as described previously (Taniguchi et al., 2024).

2.3. Measurement of biomass composition in yeast

The biomass composition of yeast cells was measured using GC-MS by following previously described methods with slight modifications (Long and Antoniewicz, 2014). Briefly, yeast cells spiked with ^{13}C-labeled internal standards were hydrolyzed and analyzed using GC-MS. In this study, protein-bound amino acids, RNA-bound ribose, polysaccharide-bound glucose and mannose, and lipid-bound fatty acids were measured in the yeast biomass. The extracted ribose, glucose, and mannose were converted to aldonitrile propionate derivatives and analyzed using GC-MS (Antoniewicz et al., 2011). The amounts of AMP, UMP, GMP, and CMP were calculated using the previously described compositional ratios (Forster et al., 2003).

2.4. Measurement of ^{13}C labeling ratios of protein-bound amino acids

The culture broth was collected to achieve OD_{600} × mL = 3.0 and centrifuged at 15000 rpm, 4 °C for 15 min. The cell pellet was resuspended in 1 mL of 0.9 % saline solution and centrifuged under the same conditions. The washing step was repeated twice. After addition of 2 mL of 6 *N* HCl, the cell suspension was heated at 105 °C for 18 h in a heat block incubator (ND-MO1, Nisshin Rika, Tokyo, Japan). The hydrolysate was filtered, and 10 μL of cycloleucine was added to 600 μL of the filtrate, which was then dried using a centrifugal evaporator (CVE-3000, EYELA, Tokyo, Japan). For amino acid derivatization, 50 μL of acetonitrile and 50 μL of *N*-methyl-*N*-(*tert*-butyldimethylsilyl)trifluoroacetamide + 1 % *tert*-butyldimethylchlorosilane (MTBSTFA+1 % TBDMCS, Thermo Fisher Scientific, Waltham, MA USA) were added to the dried sample, which was heated at 105 °C for 90 min. After cooling

to room temperature, the mixture was centrifuged at 15,000 rpm, 4 °C for 5 min, and the supernatant was subjected to GC-MS analysis (GCMS-QP2020, Shimadzu). GC-MS was performed as described previously (Okahashi et al., 2014).

2.5. Measurement of ^{13}C-labeling ratios of intracellular metabolites

Cells were collected by filtering 10 mL of culture broth at an OD_{600} of approximately 1.0. The filter was immediately immersed in 1600 μL of cool methanol. After addition of 1600 μL of chloroform (−30 °C) and 640 μL of MilliQ water (4 °C), vigorous mixing, and 1 min of sonication, the mixture was centrifuged at 2900 *g*, 4 °C, using a swing rotor for 20 min. The upper layer was collected in three Eppendorf tubes (250 μL each) and dried using a centrifugal evaporator. ^{13}C labeling of sugar phosphates was measured using the ion-pair-LC-MS analysis method. The dried samples were dissolved in 50 μL of MilliQ water and subjected to the analysis using LC-MS (LCMS-8060-NX, Shimadzu). The LC and MS conditions were as follows: Columns: MASTRO2 C18 (Shimadzu, 150 mm by 2.1 mm, pore size, 3 μm). Mobile phase A: 10 mM tributylamine, 15 mM acetic acid; mobile phase B: methanol; column temperature: 40 °C; flow rate: 0.3 mL/min; injection volume: 1 μL; gradient curve (min/B conc): 0/0, 0.5/0, 8/25, 12/98, 15/98, 15.1/0, 20/0; polarity: negative ion mode; electrospray voltage: 4.0 kV; nebulizing gas flow: 3.0 L min^{-1}; drying gas flow:15 L min^{-1}. The multiple reactions monitoring (MRM) transitions and parameters of the target compounds are listed in Supplementary Table S1. For the measurement of organic and amino acids by GC-MS, 50 μL of 40 mg/mL methoxyamine hydrochloride in pyridine was added to the dried samples, which were then stirred at 30 °C for 60 min in a Deep Well Maximizer (TAITEC). Following the addition of 50 μL of MTBSTFA +1 % TBDMCS, the mixture was stirred at 60 °C for 60 min. After cooling to room temperature for 2 h, the supernatant was subjected to GC-MS as described previously (Okahashi et al., 2022).

2.6. ^{13}C-based metabolic flux analysis

The metabolic network of *S. cerevisiae* that was established in previous studies was used (Supplementary Table S2) (Frick and Wittmann, 2005). The unlabeled fractions of inoculated cell-derived proteinogenic amino acids were corrected based on the OD_{600} at the initial and sampling times. The effects of naturally occurring isotopes were eliminated using a previously described method (van Winden et al., 2002). The fractional labeling level of each metabolite was calculated using the following equation:

$$\text{Fractional labeling } (FL) = \Sigma\,([\mathrm{M}+i] \times i / n)$$

Where n and $[\mathrm{M}+i]$ represent the number of C atoms in the carbon skeleton and the ratio of isotopomers, including i ^{13}C atom(s), respectively (Okahashi et al., 2022). The biomass equation was modified from a previous study (Forster et al., 2003). When the measured content of amino acid *AA* in the biomass was x mmol/g dry-cell weight (DCW), the newly synthesized amount of *AA* was calculated as $x \times FL$ using the measured fractional labeling value of *AA* in the protein from the [U-^{13}C] glucose culture. For unmeasured amino acids, including Cys, Met, Trp, Lys, His, and Arg, the reported biomass compositions were used (Forster et al., 2003) and *FL* was set to zero. Additionally, nucleic acids and lipids were assumed to be synthesized *de novo*. Computational analyses were performed using mfapy (Matsuda et al., 2021) (https://github.com/fumiomatsuda/mfapy). Metabolic flux distribution was estimated by minimizing the residual sum of the squares of the measured and estimated isotopic labeling patterns and effluxes. The standard deviation of ^{13}C-labeling was assumed to be 0.01. The goodness of fit was evaluated by χ^2 statistics test (Antoniewicz et al., 2006). The 95 % confidence intervals (CIs) were determined using the grid search method (Antoniewicz et al., 2006).

3. Results

3.1. Culture profile and biomass composition in synthetic and complex media

The diploid laboratory strain of *S. cerevisiae*, BY4947, was batch cultured in SD medium in a flask as a control. Exponential growth was observed from 3 to 9 h after inoculation (Fig. 1A), with a specific growth rate of 0.367 ± 0.004 h^{-1} (Fig. 1B and Supplementary Table S3). The metabolite concentrations in the medium were measured to calculate the specific rates (Supplementary Fig. S1). The specific glucose uptake rate was determined to be 14.2 ± 0.2 mmol (g DCW h)$^{-1}$. Moreover, the specific production rates of ethanol, glycerol, and acetic acid were 21.45 ± 0.27, 0.98 ± 0.02, and 0.28 ± 0.01 mmol (g DCW h)$^{-1}$, respectively (Fig. 1B and Supplementary Table S3). These results are consistent with those of previous studies conducted under identical conditions (Yatabe et al., 2021).

Cultivation tests were performed under the same conditions using SD medium supplemented with 1 mM of 20 amino acids (SD + AA medium) and YPD medium. The BY4947 strain exhibited improved growth rates (Fig. 1A), with specific growth rates of 0.438 ± 0.007 and 0.531 ± 0.004 h^{-1} in SD + AA and YPD media, respectively (Fig. 1B and Supplementary Table S3). Moreover, the final ODs reached were 5.4 ± 0.4 and 18.6 ± 0.5 in SD + AA and YPD media, respectively (Fig. 1A). This enhancement is attributed to the use of amino acids and other building blocks in the medium for biomass synthesis.

The specific glucose uptake rates in the SD + AA and YPD media were approximately 92 % and 100 % of those in the SD medium, respectively (Fig. 1B and Supplementary Table S3). In contrast, the specific ethanol production rates in the SD + AA and YPD media increased by 16 % and 21 % compared to those in the SD medium, respectively, suggesting a shift in carbon flux from biomass precursor synthesis to ethanol production. The specific glycerol and acetate production in SD + AA medium were increased by 21 % and 39 % of those in the SD medium (0.98 ± 0.02 and 0.28 ± 0.01 mmol (g DCW h)$^{-1}$), respectively (Fig. 1B and Supplementary Table S3). In the YPD medium, these rates were 0.24 ± 0.03 and 1.39 ± 0.07 mmol (g DCW h)$^{-1}$, respectively, suggesting that the production of glycerol is redirected to acetate (Fig. 1B and Supplementary Table S3). Furthermore, the YPD medium contained 1.7 ± 0.1 mM of fructose (Supplementary Fig. S1E), which was consumed by *S. cerevisiae* at a specific uptake rate of 0.59 ± 0.05 mmol (g DCW h)$^{-1}$ (Supplementary Table S4).

The effects of the cultivation conditions on the biomass composition were also investigated. The coefficients for converting OD_{600} to g DCW L^{-1} were constant among the three media (0.282 ± 0.010, 0.286 ± 0.003, and 0.294 ± 0.020 for yeast cells cultured in the SD, SD + AA, and YPD media, respectively; data not shown). The compositions of amino acids, fatty acids, RNA-bound ribose, and polysaccharide-bound glucose showed no significant differences among the yeast biomasses cultured in SD, SD + AA, and YPD media (Supplementary Table S5).

3.2. Incorporation of amino acids into the central carbon metabolism

We also investigated whether the amino acids in the SD + AA medium could be incorporated into central carbon metabolism. For this purpose, glucose in the SD + AA medium was substituted with [U-$^{13}C_6$] glucose and cultivation was carried out under the same conditions. If [U-$^{13}C_6$]glucose was the sole carbon source, all intermediates within the cells would be fully labeled with ^{13}C atoms, whereas if carbon from amino acids or other building blocks was incorporated into central metabolism, non-labeled or partially labeled intermediates would be observed. After 9 h of cultivation, the cells were harvested and intracellular metabolites were extracted for LC-MS and GC-MS analyses to determine the stable isotope labeling patterns or mass isotopomer distribution vectors (MDVs) of the central metabolic intermediates (Supplementary Fig. S2). In addition, proteins from the harvested cells

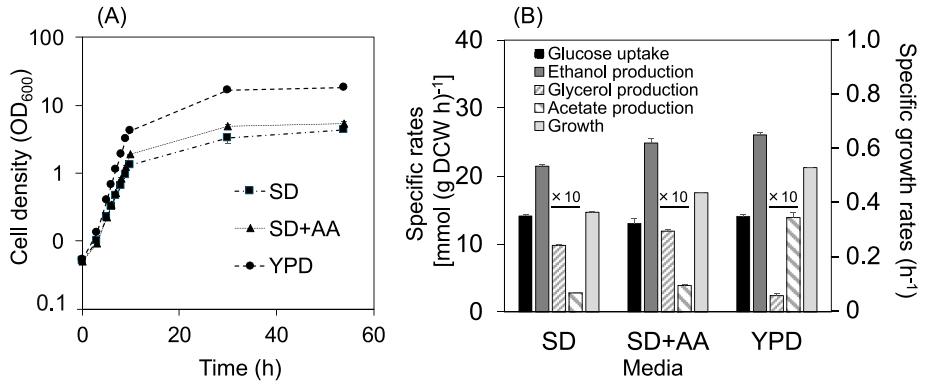

Fig. 1. Culture profiles of *S. cerevisiae* cultivated in synthetic and complex media. The BY4947 strain (diploid laboratory strain) was batch cultured on a flask-scale using synthetic dextrose (SD), SD supplemented with 1.0 mM of 20 amino acids (SD + AA), and yeast extract peptone dextrose (YPD) media. (A) Time course of cell density. (B) Specific rates for glucose uptake, ethanol, glycerol, acetate production and cell growth. The "x10" indicates that the values are expressed as 10 times. The data are presented as mean ± standard deviation (n = 3).

were hydrolyzed, derivatized, and subjected to GC-MS analysis to measure the MDVs of the protein-derived amino acids (Supplementary Fig. S3).

We then calculated the fractional labeling (fraction of ^{13}C-labeled atoms) from the measured labeling patterns. For example, the fractional labeling of glucose-6-phosphate (G6P) was close to 1.0 (Fig. 2A) because most of the total G6P pool was an [M+6] isotopomers containing six ^{13}C atoms (Supplementary Fig. S2). High fractional labeling values were observed for all intermediates in the glycolysis and pentose phosphate (PP) pathways (Fig. 2A), indicating predominant synthesis from [U-^{13}C] glucose and minimal entry of carbon from the assimilated amino acids into glycolysis. Similar high fractional labeling values were observed in the YPD medium (Fig. 2A).

In contrast, TCA cycle intermediates showed a decrease in fractional labeling (Fig. 2A). For example, the fraction labeling ratios of citrate (Cit) and α-ketoglutarate (aKG) were 0.54 and 0.16, respectively (Fig. 2A). As Glu and Gln are biosynthesized from aKG, we compared the ^{13}C labeling patterns of free intracellular aKG and protein-derived Glx. In this study, Glx indicates a mixture of Glu and Gln because Gln is converted into Glu during acid hydrolysis of the protein. The labeling pattern of protein-bound Glx closely resembled that of free aKG (Fig. 2B). These results suggest that following uptake from the medium, Gln and Glu are rapidly interconverted with intracellular aKG via transamination reactions in yeast cells. Thus, a portion of the carbon from Gln or Glu is incorporated into the TCA cycle.

Next, we considered whether Asp and Asn are biosynthesized from oxaloacetate (OAA). Although OAA was not detectable using our method of analysis, OAA and malate were converted by a reversible reaction and were therefore expected to exhibit a similar labeling pattern. The labeling patterns of protein-derived Asx (the Asp/Asn mixture) resembled those of intracellular malate (Fig. 2C). This suggests that, similar to Glu and Gln, Asp and Asn were incorporated into the TCA cycle. Similar trends were observed in cells cultivated in the YPD medium (Supplementary Fig. S4).

Next, we compared the fractional labeling of protein-derived amino acids in cells cultivated in the SD + AA medium containing [U-$^{13}C_6$] glucose (Fig. 2D). In this study, the labeling patterns of six amino acids (Cys, Met, Trp, Lys, His, and Arg) were not measured because of their instability during acid hydrolysis and because of interfering signals in the GC-MS analysis. The results for the other 14 amino acids revealed that the fractional labeling values varied considerably among the different amino acids. For instance, Phe, Tyr, and Thr exhibited very low fractional labeling, indicating that these amino acids in proteins were predominantly derived from extracellular uptake, with negligible *de*

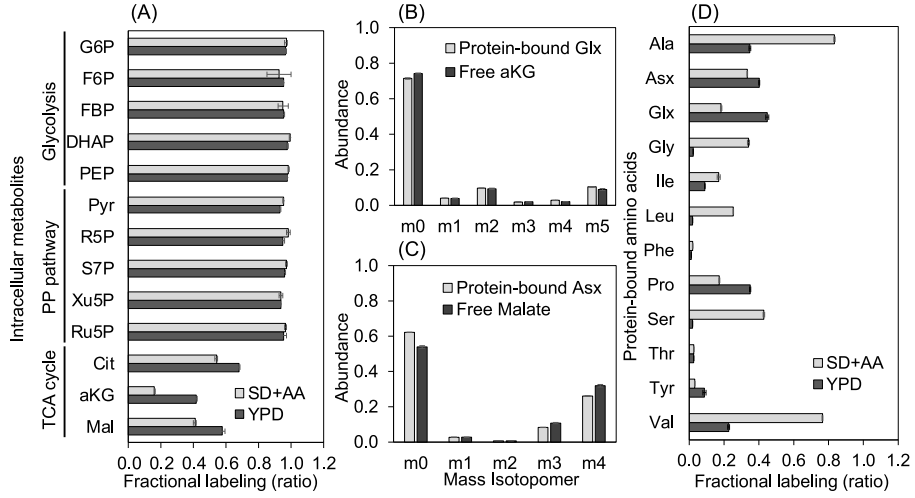

Fig. 2. The labeling patterns of intracellular metabolites and protein-bound amino acids in cells cultivated in SD + AA and YPD medium containing [U-$^{13}C_6$]glucose. The cells were harvested after 9 h of cultivation. (A) Fractional labeling of intracellular metabolites. (B, C) Mass isotopomer distributions of (B) protein-bound Glx and free aKG and (C) protein-bound Asx and free Mal in the cells cultivated in the SD + AA medium. The labels on the x-axis (m0, m1, m2, etc.) represent the numbers of ^{13}C atoms in each isotopomer. (D) Fractional labeling of protein-bound amino acids. Fractional labeling levels (the fraction of ^{13}C-labeled atoms) were calculated from the mass isotopomer distribution data shown in Supplementary Figs. S2 and S3. The data are presented as mean ± standard deviation (n = 3).

novo biosynthesis. In contrast, Ala and Val showed relatively high fractional labeling levels of approximately 0.8, because the pools of these amino acids contained both non-labeled and fully ^{13}C-labeled isotopomers. This suggests that the Ala and Val used for protein synthesis were a mixture of extracellularly assimilated and *de novo* synthesized fractions. Interestingly, the analysis of cells cultivated in YPD medium showed that the fractional labeling values differed markedly from those observed in SD + AA medium (Fig. 2D). This discrepancy may arise from variations in the concentration of each amino acid between media (Supplementary Fig. S5). This observation supports that the composition of the growth medium affects the dependence of protein synthesis on extracellularly supplied amino acids.

The very low fractional labeling of Phe, Tyr, and Thr in the SD + AA and YPD media suggests that *S. cerevisiae* utilizes extracellularly supplied these amino acids when they are supplied in the medium, probably because *de novo* biosynthesis of these amino acids is costly. Thus, the utilization of extracellularly supplied amino acids contributed to the faster growth of *S. cerevisiae* in SD + AA and YPD media. However, there are no single bottleneck amino acids that are particularly expensive to biosynthesize because it has been reported that the supplementation of one of the amino acids was not sufficient to improve cell growth (Hanscho et al., 2012).

3.3. Comparison of the uptake rate and demand for biomass synthesis of Gln, Glu, Asp, and Asn

The ^{13}C labeling experiments indicated that the cells co-utilized Gln, Glu, Asp, Asn, and glucose as carbon sources in the SD + AA medium. To confirm this finding, the Gln and Glu contents of the media were monitored to determine their specific uptake rates. In the SD + AA medium, the levels of Gln and Glu decreased in a time-dependent manner but did not reach zero even after 54 h (Supplementary Fig. S5). The specific uptake rates of Glu and Gln were estimated to be 0.066 ± 0.031 and 0.126 ± 0.024 mmol (g DCW h)$^{-1}$, respectively (Supplementary Table S4). The sum uptake rate of Gln and Glu was estimated to be 0.192 mmol (g DCW h)$^{-1}$, which accounted for 1.5 % of the glucose uptake rate. The uptake rate was compared with the amounts of Glu and Gln required for protein biosynthesis. The Glx content in yeast biomass cultured in SD + AA medium was 0.756 ± 0.094 mmol (g DCW)$^{-1}$ (Supplementary Table S5). The specific growth rate was 0.438 ± 0.007 h^{-1} (Fig. 1B), and the fraction of non-labeled protein-bound Glx was 0.82 (Fig. 2D). This indicates that the amount of medium-derived Glx required for biomass synthesis was 0.270 mmol (g DCW h)$^{-1}$, which is close to the sum of the uptake rates of Glu and Gln (Fig. 3). A similar equivalence was observed for Asp and Asn in both SD + AA and YPD medium (Fig. 3). The Gln uptake rate was not measured because the Gln level in the YPD medium was below the detection limit (Supplementary Fig. S5). In contrast, the uptake rate of Glu in the YPD medium was higher than that required for biomass synthesis, suggesting that excess Glu was incorporated into the TCA cycle. Despite significant uptake, the uptake rates of Gln, Glu, Asp, and Asn were much lower than that of glucose. Thus, these results indicate that the net amount of carbon incorporated into the TCA cycle was relatively low, while Glx and Asx taken up by the cells were rapidly interconverted with aKG and OAA within the cells.

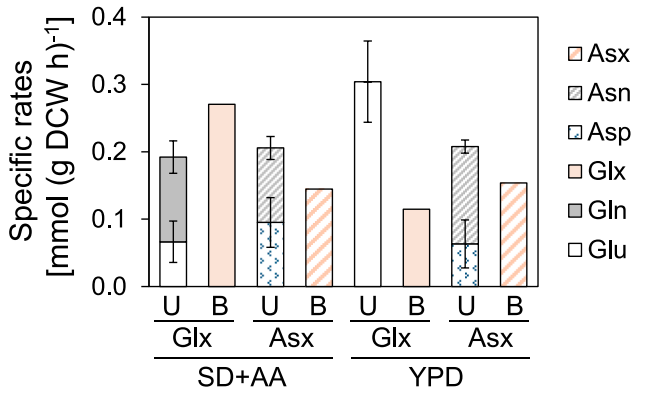

Fig. 3. Specific uptake rates of glutamate (Glu), glutamine (Gln), aspartate (Asp), and asparagine (Asn) and their consumption rates for the biomass synthesis. The letters indicate uptake (U) and consumption for biomass synthesis (B). The data are presented as mean ± standard deviation (n = 3).

3.4. ^{13}C-MFA of S. cerevisiae in SD + AA and YPD media

Based on these insights, ^{13}C-MFA was conducted on *S. cerevisiae* cultured in SD + AA and YPD media. As a control, the metabolic flux distribution in SD medium was estimated (Supplementary Data S1). *S. cerevisiae* cells were cultured under identical conditions in SD medium with [1–^{13}C]glucose as the sole carbon source. Three replicates were performed for the main culture, from which the cells were harvested during the mid-log phase. Amino acids obtained from the acid hydrolysis of cellular proteins were derivatized using TDBMS, and the MDVs of each amino acid were measured using GC-MS. ^{13}C-MFA was performed using the specific rates and MDV data (Supplementary Tables S3 and S6). A previously established metabolic model comprising glycolysis, the TCA cycle, and oxidative pentose phosphate (oxPP), anaplerotic, and ethanol biosynthesis pathways was used (Supplementary Table S2).

The results of ^{13}C-MFA are shown in Fig. 4A, Supplementary Data S1, and Supplementary Table S7. Out of the glucose uptake rate of 14.9 mmol (g DCW h)$^{-1}$, approximately 9 % (1.3 mmol (g DCW h)$^{-1}$) of glucose-6-phosphate (G6P) entered the oxPP pathway. This pathway regenerates NADPH, which is utilized for synthesizing building blocks such as amino acids. Most of the remaining G6P was converted into pyruvate via glycolysis, which was then utilized for ethanol biosynthesis. Additionally, the metabolic flux level of the anapletotic pathway, which generates OAA from pyruvate, was determined to be 1.3 mmol (g DCW h)$^{-1}$. This pathway supplies the carbon necessary for amino acid synthesis from aKG and OAA, including Glu, Glu, Asp, and Asn. Meanwhile, the flux entering the TCA cycle from acetyl-CoA was found to be 0.4 mmol (g DCW h)$^{-1}$. This flux distribution closely resembles the results reported in a previous study (Yatabe et al., 2021).

The metabolic flux distribution in the SD + AA medium was also investigated. For parallel labeling, *S. cerevisiae* was cultured in two variations of SD + AA medium containing [1–^{13}C]glucose or [U-$^{13}C_6$] glucose. As shown in Fig. 4B, [1–^{13}C]glucose is useful for measuring the branching ratio between the Embden Meyerhof Parnas (EMP) pathway (red arrow) and the oxPP pathway (blue arrows). This is because the [1–^{13}C]-labeled and non-labeled forms of pyruvate are produced via the EMP pathway, whereas the oxPP pathway produces only the non-labeled form of pyruvate. The branching ratio can be determined from the ^{13}C labeling patterns of amino acids derived from pyruvate. [U-$^{13}C_6$] glucose was also used to determine the contributions of other carbon sources such as Glx (Fig. 4C).

Cells were harvested during the mid-log phase to extract intracellular metabolites. The crude extract of intracellular metabolites was divided and used for two analytical methods to measure MDVs: one for sugar phosphates using ion-pairing LC-MS and the second for organic acids and amino acids using GC-MS with chemical derivatization (Supplementary Table S8). The metabolic model was modified to account for Glx and Asx uptake (Supplementary Table S2). The equation representing biomass synthesis in the metabolic model was modified by calculating the amount of newly synthesized amino acids required for biomass synthesis using fractional labeling data (Fig. 2D) (Forster et al., 2003). It was assumed that other building blocks such as lipids and nucleotides were synthesized *de novo*. Using the two sets of MDV data, the modified metabolic model, and measured uptake rates of Glx and Asx (Fig. 3), a metabolic flux distribution passing the χ^2 statistics test

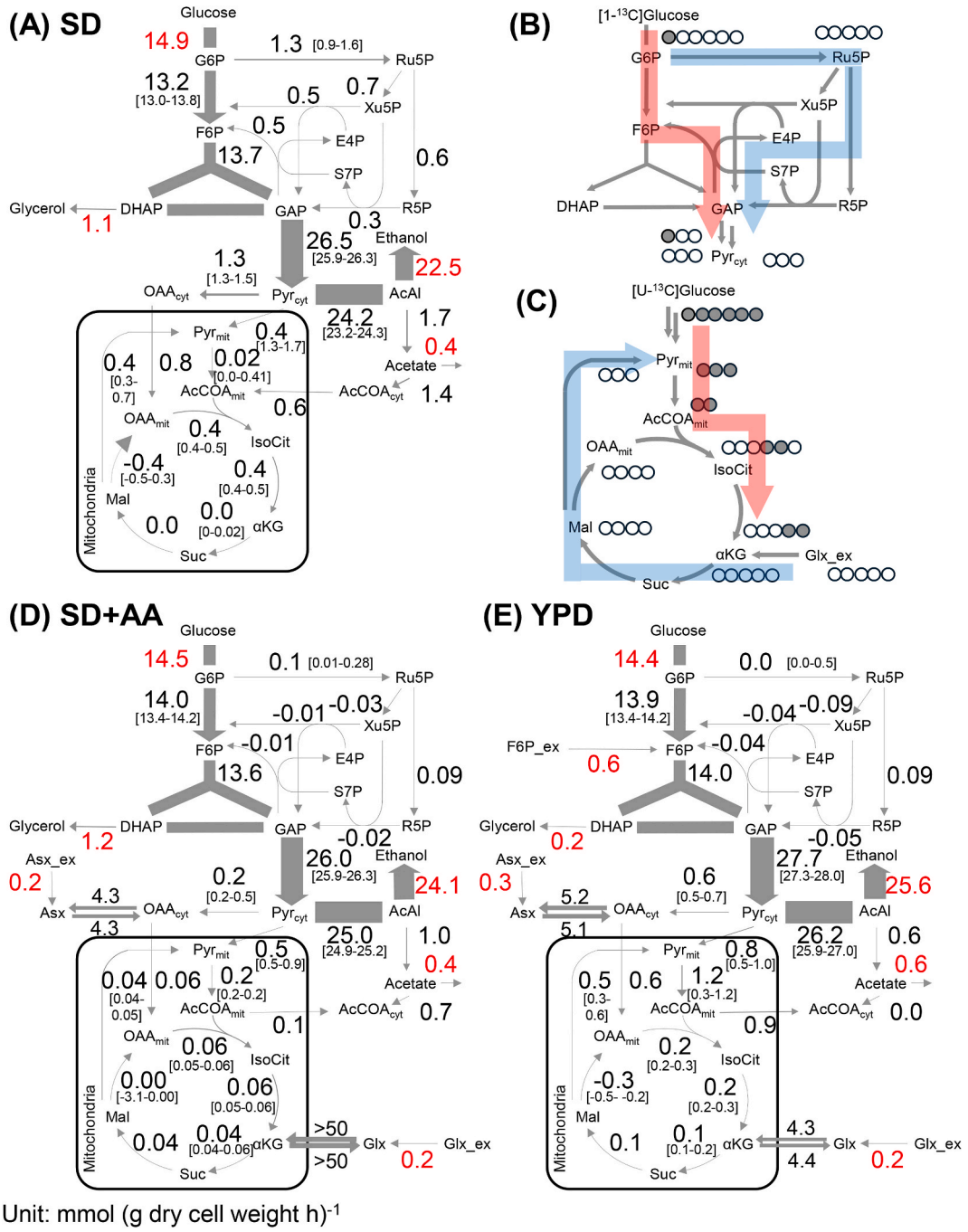

Fig. 4. Metabolic flux distributions (mmol (g DCW h)$^{-1}$) of *S. cerevisiae* in different media. (A) Flux values in the central carbon metabolism of *S. cerevisiae* cultivated in SD with 95 % confidence intervals. (B and C) Transfer of ^{13}C atoms (closed circle) in the labeling experiment using [1–^{13}C]glucose (B) and [U-^{13}C]glucose (C). Representative isotopomers are shown in simplified metabolic pathways. (D and E) Flux values of *S. cerevisiae* cultivated in SD + AA (D) and YPD (E). The width of each arrow indicates the best-fit value. Values estimated from specific rates are shown in red. These flux values are shown in Supplementary Data S1-S3.

was estimated by using the parallel labeling method (Supplementary Table S7 and Supplementary Data S2).

Fig. 4D shows the metabolic flux distribution in the SD + AA medium. The glucose consumption rate of 14.5 mmol (gDCW h)$^{-1}$ was almost identical to that of the SD medium. However, the proportion of G6P entering the oxPP pathway decreased to 0.1 mmol (gDCW h)$^{-1}$. The 95 % confidence intervals of the metabolic flux level of the oxPP pathway (0.01–0.28 mmol (gDCW h)$^{-1}$)) did not overlap with that in the SD medium (0.9–1.6 mmol (gDCW h)$^{-1}$)), supporting a significant reduction in the metabolic flux of the oxPP pathway (Fig. 4A and D). This was probably because the amount of NADPH required for amino acid synthesis decreased due to the uptake of amino acids from the medium. Additionally, assimilated Glx and Asx were rapidly interconverted with aKG and OAAcyt within the cells. However the metabolic flux of the TCA cycle remained low because the net influx into the TCA cycle was close to zero (Figs. 3 and 4D). The metabolic flux level of the anaplerotic pathway decreased to 0.2 mmol (gDCW h)$^{-1}$, which was approximately one-third of that in the SD medium. This is likely due to the decreased need for anaplerosis for amino acid synthesis. With the decrease in flux level in these branching pathways, the flux for ethanol production reached 24.1 mmol (gDCW h)$^{-1}$.

The metabolic flux distribution in cells cultivated in the YPD medium

was estimated using a method similar to that used for the SD + AA medium. Reactions for fructose uptake were added to the metabolic model because fructose uptake occurred in the YPD medium (Supplementary Table S2). The estimated flux distribution (Fig. 4E and Supplementary Data S3) showed that the 95 % intervals of the metabolic flux estimations of the oxPP pathway and anaplerotic reactions were 0.0–0.5 and 0.5–0.7 mmol (gDCW h)$^{-1}$, respectively, which were significantly lower than those of the SD medium (Fig. 4A). While the NADPH supply from the oxPP pathway was close to zero, other reactions, such as $NADP^+$-dependent aldehyde dehydrogenase (ALD, AcAl + $NADP^+$ => Acetate + NADPH), could supply NADPH (Fig. 4E) (Saint-Prix et al., 2004). The metabolic flux levels of the ALD reaction in the SD + AA and YPD media were 1.0 and 0.6 mmol (gDCW h)$^{-1}$, respectively (Fig. 4D and E). Furthermore, the specific ethanol production rate increased to 25.6 mmol (gDCW h)$^{-1}$, which is likely due to a further reduction in *de novo* amino acid biosynthesis.

These results demonstrate that ^{13}C-MFA of *S. cerevisiae* in complex media was achieved by parallel labeling and measurement of amino acid uptake rates. ^{13}C-MFA of *S. cerevisiae* in YPD medium revealed that the metabolic fluxes through the oxPP and anaplerotic pathways, which supply NADPH and precursors for amino acid biosynthesis, were smaller than those in SD medium.

3.5. ^{13}C-MFA of *S. cerevisiae* in malt extract (ME) medium

To validate the developed approach, the established method was applied to ^{13}C-MFA of *S. cerevisiae* cultivated in malt extract (ME) medium containing malt extract supplemented with glucose. Cells of *S. cerevisiae* were cultured in the ME medium using identical conditions (Fig. 5A), from which the specific growth rate during the log phase was determined to be 0.497 ± 0.011 h^{-1} (Supplementary Table S3). Additionally, the specific rates of glucose consumption and ethanol, glycerol, and acetate production were determined using medium component analysis (Fig. 5B). The analysis also revealed that fructose consumption was similar to that in YPD medium (Supplementary Fig. S1 and Table S4). However, maltose consumption in the medium was not observed until 54 h of cultivation (Supplementary Fig. S6). This was likely due to catabolite repression by glucose and the weak maltose utilization capability of the BY4947 strain (Hatanaka et al., 2018; Ohdate et al., 2018). Furthermore, the fractional labeling of intracellular metabolites was calculated from their labeling patterns in ME medium containing [U-^{13}C]glucose (Supplementary Figs. S2, S3, and S7). This result was similar to that obtained with the YPD medium, because the entry of amino acids into glycolysis was minimal, whereas there were significant levels of incorporation of Glx and Asx into the TCA cycle (Supplementary Fig. S4). The biomass composition of the cells cultured in ME was considered identical to that of YPD because of the small variance among the culture conditions (Supplementary Table S5). Fractional labeling data for protein-derived amino acids (Supplementary Fig. S7) were used to update the biomass equation in the metabolic model (Supplementary Table S2). A statistically acceptable metabolic flux distribution was estimated (Fig. 5C, Supplementary Table S7, and Supplementary Data S4) that was similar to that in the YPD medium (Fig. 4C). The metabolic flux levels of the oxPP pathway and anaplerotic reactions were 0.1 and 0.5 mmol (gDCW h)$^{-1}$, respectively, and the specific ethanol production rate was 24.6 mmol (gDCW h)$^{-1}$, which is slightly lower than that in YPD medium. This likely reflects an increase in *de novo* amino acid biosynthesis compared to that in YPD medium.

4. Discussion

In this study, we investigated a method to estimate the metabolic flux distribution of *S. cerevisiae* in complex media. *S. cerevisiae* cells were cultured in SD + AA, YPD, and ME media containing [U-^{13}C]glucose (Fig. 1). ^{13}C-labeling of intracellular metabolites was performed to confirm the incorporation of other carbons into the central metabolism (Fig. 2). These results suggest that Glu, Gln, Asp, and Asn were taken up from the medium and fed into the TCA cycle (Fig. 2). The fractional labeling ratio of protein-bound amino acids was measured in *S. cerevisiae* cultured in a complex medium containing [U-$^{13}C_6$]glucose (Fig. 2D).

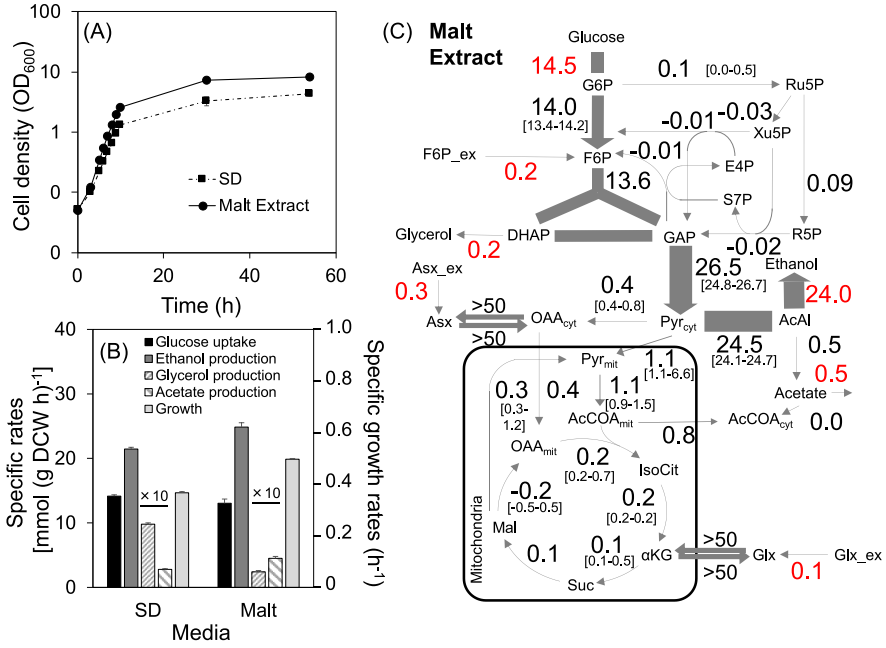

Fig. 5. ^{13}C-Metabolic flux analysis of *S. cerevisiae* cultivated in malt extract (ME) medium. (A) Time course of cell density. (B) Specific rates for cell growth, glucose uptake, ethanol, glycerol, and acetate production. Results were compared with those of the SD medium shown in Fig. 1. The "x10" indicates that the values are expressed as 10 times. The data are presented as mean ± standard deviation (n = 3). (C) Metabolic flux distributions (mmol (g DCW h)$^{-1}$) of *S. cerevisiae* in the ME medium. Flux values in the central carbon metabolism are shown with 95 % confidence intervals. The width of each arrow indicates the best-fit value. Values estimated from specific rates are shown in red. These flux values are shown in Supplementary Data S4.

Fractional labeling data enabled the amount of newly synthesized amino acids required for biomass production to be to be quantified. Moreover, component analysis of the media revealed the consumption of fructose in YPD and ME (Supplementary Fig. S1). Based on these findings, a specific metabolic model was created for SD + AA,YPD, and ME media by the modification of the biomass equation and the addition of uptake reactions for additional carbon sources. (Supplementary Table S2).

Previous studies have shown that aspartate serves as a carbon source for trehalose synthesis in *S. cerevisiae* under gluconeogenic conditions (Varahan et al., 2020). Furthermore, aKG can be transported, catabolized, and used for biomass synthesis at low pH (Zhang et al., 2020). It was also reported that proteomic reallocation from amino acid biosynthesis to ribosomes was responsible for faster growth in complex media (Bjorkeroth et al., 2020). This study showed that *S. cerevisiae* simultaneously utilizes Glu, Gln, Asp, and Asn as carbon sources in parallel with glucose under commonly used conditions, such as aerobic batch cultures in YPD medium (Fig. 2). The parallel consumption of glucose and glutamine as carbon sources has been observed in cancer cells and is considered a hallmark of cancer-specific metabolism (Yang et al., 2017). It has been reported that the overexpression of Pdp3 in *S. cerevisiae* causes changes in metabolic profiles such as glutaminolysis (Rona et al., 2019). This study provided more direct evidence of glutamine utilization by *S. cerevisiae* using the ^{13}C labeling experiment (Fig. 2). The existence of a similar glutaminolysis-like metabolism in *S. cerevisiae* is intriguing because *S. cerevisiae* and tumors commonly display enhanced glycolytic activity and impaired oxidative phosphorylation (Diaz-Ruiz et al., 2011).

Similar to a previous ^{13}C-MFA study of other organisms in complex media (Schwechheimer et al., 2018a, 2018b), the developed method depends on parallel labeling and consideration of amino acid uptake rates. Therefore, this method has certain intrinsic limitations. First, other amino acids and sugars in the medium may be incorporated into the pyruvate and acetyl-CoA pools. For example, serine and threonine affect the lifespan because they are utilized as carbon sources under glucose-depleted conditions (Kawamukai et al., 2023; Maruyama et al., 2016). This study showed that *S. cerevisiae* utilized fructose in YPD and ME (Figs. 4 and 5). Moreover, complex media often contain vitamins and trace elements that affect the metabolic flux. This condition dependency indicates that the fractional labeling ratios and entry of other carbon sources into the central metabolism should be confirmed by labeling experiments when analyzing other cultivation conditions. Furthermore, cells can incorporate lipids and nucleic acids from the medium as building blocks. Measuring the fractional labeling ratios of these compounds can provide a more accurate flux distribution. However, the improvement in flux estimation is expected to be limited because statistically acceptable results were obtained by considering only amino acid incorporation.

^{13}C-MFA of *S. cerevisiae* in SD + AA, YPD, and ME media revealed that the carbon flow toward ethanol production via glycolysis was elevated because carbon loss by the branching pathways decreased (Figs. 4 and 5). The increase in glycolytic flux enhances ATP regeneration through substrate-level phosphorylation and contributes to the faster growth of *S. cerevisiae* in complex media. Indeed, *S. cerevisiae* in the SD + AA, YPD, and ME media showed increased cell growth rate and final OD_{600}, which could contribute to the total increase in ethanol production. ^{13}C-MFA also showed that metabolic fluxes through the oxidative pentose phosphate (oxPP) and anaplerotic pathways were significantly reduced in the complex media (Figs. 4 and 5). The reduced anaplerotic pathway flux level could be explained by the uptake of Glu, Gln, Asp, and Asn from the medium and their feeding into the TCA cycle (Fig. 2). However, the regulatory mechanisms underlying amino acid assimilation remain unclear. The reduction in oxPP flux seems to reflect a decrease in the need for NADPH required for amino acid biosynthesis. This hypothesis should be confirmed in the future by measuring NADPH levels and performing enzymatic assays considering the redox balance in *S. cerevisiae*.

As mentioned in the Introduction, ^{13}C-MFA is an important tool in metabolic engineering and process optimization (Wiechert, 2001). Such applications require precise measurements of metabolic flux distributions under various culture conditions including complex media. This study demonstrated an approach for ^{13}C-MFA of *S. cerevisiae* cultivated in YPD and ME media. To extend this approach to other complex media, this study indicated that modification of the biomass equation and consideration of additional carbon sources are necessary for each medium. This can be accomplished through component analysis of the medium and measurement of the fractional labeling ratios of protein-bound amino acids. By further developing this method, the metabolic fluxes of engineered *S. cerevisiae* strains in complex media, as well as those of industrial *S. cerevisiae* strains under production conditions, can be analyzed at the flux level. Parallel labeling experiments using other carbon sources, including ^{13}C labeled acetate and amino acids, would reduce overlap and improve the accuracy of flux distribution across pathways. A time-resolved ^{13}C-MFA across different growth phases would capture dynamic shifts in flux distributions in response to nutrient and oxygen availability. ^{13}C-MFA of *S. cerevisiae* cultured in complex media provides valuable insights into metabolic engineering and process optimization in industrial yeast fermentation.

CRediT authorship contribution statement

Hayato Fujiwara: Validation, Investigation. **Nobuyuki Okahashi:** Writing – original draft, Validation, Methodology, Investigation. **Taisuke Seike:** Validation, Investigation. **Fumio Matsuda:** Writing – review & editing, Methodology, Conceptualization.

Funding

This work was supported in part by Grants in Aid for Scientific Research (B) (22H01879) and JST, CREST (Grant Number JPMJCR21N2), Japan.

Declaration of competing interest

The authors declare that they have no known competing financial interests or personal relationships that could have appeared to influence the work reported in this paper.

Acknowledgments

We thank Drs. Qiuyi Wang, Yuki Ito, and Junko Iida from the Shimadzu Corporation for their helpful comments and technical assistance.

Appendix A. Supplementary data

Supplementary data to this article can be found online at https://doi.org/10.1016/j.mec.2025.e00260.

Data availability

Data will be made available on request.

References

Adler, P., Bolten, C.J., Dohnt, K., Hansen, C.E., Wittmann, C., 2013. Core fluxome and metafluxome of lactic acid bacteria under simulated cocoa pulp fermentation conditions. Appl. Environ. Microbiol. 79, 5670–5681.

Antoniewicz, M.R., 2015. Methods and advances in metabolic flux analysis: a mini-review. J. Ind. Microbiol. Biotechnol. 42, 317–325.

Antoniewicz, M.R., Kelleher, J.K., Stephanopoulos, G., 2006. Determination of confidence intervals of metabolic fluxes estimated from stable isotope measurements. Metab. Eng. 8, 324–337.

Antoniewicz, M.R., Kelleher, J.K., Stephanopoulos, G., 2011. Measuring deuterium enrichment of glucose hydrogen atoms by gas chromatography/mass spectrometry. Anal. Chem. 83, 3211–3216.

Bjorkeroth, J., Campbell, K., Malina, C., Yu, R., Di Bartolomeo, F., Nielsen, J., 2020. Proteome reallocation from amino acid biosynthesis to ribosomes enables yeast to grow faster in rich media. Proc. Natl. Acad. Sci. U. S. A. 117, 21804–21812.
Blank, L.M., Kuepfer, L., Sauer, U., 2005. Large-scale ^{13}C-flux analysis reveals mechanistic principles of metabolic network robustness to null mutations in yeast. Genome Biol. 6, R49.
Boone, C., 2014. Yeast systems biology: our best shot at modeling a cell. Genetics 198, 435–437.
Borodina, I., Nielsen, J., 2014. Advances in metabolic engineering of yeast *Saccharomyces cerevisiae* for production of chemicals. Biotechnol. J. 9, 609–620.
Christen, S., Sauer, U., 2011. Intracellular characterization of aerobic glucose metabolism in seven yeast species by ^{13}C flux analysis and metabolomics. FEMS Yeast Res. 11, 263–272.
Costenoble, R., Muller, D., Barl, T., van Gulik, W.M., van Winden, W.A., Reuss, M., Heijnen, J.J., 2007. ^{13}C-Labeled metabolic flux analysis of a fed-batch culture of elutriated *Saccharomyces cerevisiae*. FEMS Yeast Res. 7, 511–526.
Diaz-Ruiz, R., Rigoulet, M., Devin, A., 2011. The Warburg and Crabtree effects: on the origin of cancer cell energy metabolism and of yeast glucose repression. Biochim. Biophys. Acta 1807, 568–576.
Eliodorio, K.P., Cunha, G., Lino, F.S.O., Sommer, M.O.A., Gombert, A.K., Giudici, R., Basso, T.O., 2023. Physiology of *Saccharomyces cerevisiae* during growth on industrial sugar cane molasses can be reproduced in a tailor-made defined synthetic medium. Sci. Rep. 13, 10567.
Forster, J., Famili, I., Fu, P., Palsson, B.O., Nielsen, J., 2003. Genome-scale reconstruction of the *Saccharomyces cerevisiae* metabolic network. Genome Res. 13, 244–253.
Frick, O., Wittmann, C., 2005. Characterization of the metabolic shift between oxidative and fermentative growth in *Saccharomyces cerevisiae* by comparative ^{13}C flux analysis. Microb. Cell Fact. 4, 30.
Ghosh, A., Ando, D., Gin, J., Runguphan, W., Denby, C., Wang, G., Baidoo, E.E., Shymansky, C., Keasling, J.D., Garcia Martin, H., 2016. ^{13}C metabolic flux analysis for systematic metabolic engineering of *S. cerevisiae* for overproduction of fatty acids. Front. Bioeng. Biotechnol. 4, 76.
Hackett, S.R., Zanotelli, V.R., Xu, W., Goya, J., Park, J.O., Perlman, D.H., Gibney, P.A., Botstein, D., Storey, J.D., Rabinowitz, J.D., 2016. Systems-level analysis of mechanisms regulating yeast metabolic flux. Science 354.
Hahn-Hagerdal, B., Karhumaa, K., Larsson, C.U., Gorwa-Grauslund, M., Gorgens, J., van Zyl, W.H., 2005. Role of cultivation media in the development of yeast strains for large scale industrial use. Microb. Cell Fact. 4, 31.
Hanscho, M., Ruckerbauer, D.E., Chauhan, N., Hofbauer, H.F., Krahulec, S., Nidetzky, B., Kohlwein, S.D., Zanghellini, J., Natter, K., 2012. Nutritional requirements of the BY series of *Saccharomyces cerevisiae* strains for optimum growth. FEMS Yeast Res. 12, 796–808.
Hatanaka, H., Mitsunaga, H., Fukusaki, E., 2018. Inhibition of *Saccharomyces cerevisiae* growth by simultaneous uptake of glucose and maltose. J. Biosci. Bioeng. 125, 52–58.
Hayakawa, K., Kajihata, S., Matsuda, F., Shimizu, H., 2015. ^{13}C-metabolic flux analysis in *S*-adenosyl-L-methionine production by *Saccharomyces cerevisiae*. J. Biosci. Bioeng. 120, 532–538.
Hayakawa, K., Matsuda, F., Shimizu, H., 2018. ^{13}C-metabolic flux analysis of ethanol-assimilating *Saccharomyces cerevisiae* for *S*-adenosyl-L-methionine production. Microb. Cell Fact. 17, 82.
Kajihata, S., Matsuda, F., Yoshimi, M., Hayakawa, K., Furusawa, C., Kanda, A., Shimizu, H., 2015. ^{13}C-based metabolic flux analysis of *Saccharomyces cerevisiae* with a reduced Crabtree effect. J. Biosci. Bioeng. 120, 140–144.
Kawamukai, A., Iwano, A., Shibata, M., Kishi, Y., Matsuura, A., 2023. Serine metabolism contributes to cell survival by regulating extracellular pH and providing an energy source in *Saccharomyces cerevisiae*. Yeast 40, 59–67.
Kim, J., Kim, K.H., 2017. Effects of minimal media vs. complex media on the metabolite profiles of *Escherichia coli* and *Saccharomyces cerevisiae*. Process Biochem. 57, 64–71.
Legras, J.L., Merdinoglu, D., Cornuet, J.M., Karst, F., 2007. Bread, beer and wine: *Saccharomyces cerevisiae* diversity reflects human history. Mol. Ecol. 16, 2091–2102.
Lian, J., Mishra, S., Zhao, H., 2018. Recent advances in metabolic engineering of *Saccharomyces cerevisiae*: new tools and their applications. Metab. Eng. 50, 85–108.
Long, C.P., Antoniewicz, M.R., 2014. Quantifying biomass composition by gas chromatography/mass spectrometry. Anal. Chem. 86, 9423–9427.
Maruyama, Y., Ito, T., Kodama, H., Matsuura, A., 2016. Availability of amino acids extends chronological lifespan by suppressing hyper-aAcidification of the environment in *Saccharomyces cerevisiae*. PLoS One 11, e0151894.
Matsuda, F., Maeda, K., Taniguchi, T., Kondo, Y., Yatabe, F., Okahashi, N., Shimizu, H., 2021. mfapy: an open-source Python package for ^{13}C-based metabolic flux analysis. Metab Eng Commun 13, e00177.
Mustacchi, R., Hohmann, S., Nielsen, J., 2006. Yeast systems biology to unravel the network of life. Yeast 23, 227–238.
Nielsen, J., 2019. Yeast systems biology: model organism and cell factory. Biotechnol. J. 14, e1800421.
Nookaew, I., Olivares-Hernandez, R., Bhumiratana, S., Nielsen, J., 2011. Genome-scale metabolic models of *Saccharomyces cerevisiae*. Methods Mol. Biol. 759, 445–463.
Ohdate, T., Omura, F., Hatanaka, H., Zhou, Y., Takagi, M., Goshima, T., Akao, T., Ono, E., 2018. *MAL73*, a novel regulator of maltose fermentation, is functionally impaired by single nucleotide polymorphism in sake brewing yeast. PLoS One 13, e0198744.
Okahashi, N., Kajihata, S., Furusawa, C., Shimizu, H., 2014. Reliable metabolic flux estimation in *Escherichia coli* central carbon metabolism using intracellular free amino acids. Metabolites 4, 408–420.
Okahashi, N., Yamada, Y., Iida, J., Matsuda, F., 2022. Isotope calculation gadgets: a series of software for isotope-tracing experiments in Garuda platform. Metabolites 12, 646.
Pitkanen, J.P., Aristidou, A., Salusjarvi, L., Ruohonen, L., Penttila, M., 2003. Metabolic flux analysis of xylose metabolism in recombinant Saccharomyces cerevisiae using continuous culture. Metab. Eng. 5, 16–31.
Rona, G.B., Almeida, N.P., Santos, G.C., Fidalgo, T.K.S., Almeida, F.C.L., Eleutherio, E.C. A., Pinheiro, A.S., 2019. H NMR metabolomics reveals increased glutaminolysis upon overexpression of NSD3s or Pdp3 in. J. Cell. Biochem. 120, 5377–5385.
Saint-Prix, F., Bonquist, L., Dequin, S., 2004. Functional analysis of the ALD gene family of Saccharomyces cerevisiae during anaerobic growth on glucose: the $NADP^+$-dependent Ald6p and Ald5p isoforms play a major role in acetate formation. Microbiology (Read.) 150, 2209–2220.
Schwechheimer, S.K., Becker, J., Peyriga, L., Portais, J.C., Sauer, D., Muller, R., Hoff, B., Haefner, S., Schroder, H., Zelder, O., Wittmann, C., 2018a. Improved riboflavin production with *Ashbya gossypii* from vegetable oil based on ^{13}C metabolic network analysis with combined labeling analysis by GC/MS, LC/MS, 1D, and 2D NMR. Metab. Eng. 47, 357–373.
Schwechheimer, S.K., Becker, J., Peyriga, L., Portais, J.C., Wittmann, C., 2018b. Metabolic flux analysis in *Ashbya gossypii* using ^{13}C-labeled yeast extract: industrial riboflavin production under complex nutrient conditions. Microb. Cell Fact. 17, 162.
Schwechheimer, S.K., Becker, J., Wittmann, C., 2018c. Towards better understanding of industrial cell factories: novel approaches for ^{13}C metabolic flux analysis in complex nutrient environments. Curr. Opin. Biotechnol. 54, 128–137.
Sonderegger, M., Jeppsson, M., Hahn-Hagerdal, B., Sauer, U., 2004. Molecular basis for anaerobic growth of Saccharomyces cerevisiae on xylose, investigated by global gene expression and metabolic flux analysis. Appl. Environ. Microbiol. 70, 2307–2317.
Stewart, B.J., Navid, A., Turteltaub, K.W., Bench, G., 2010. Yeast dynamic metabolic flux measurement in nutrient-rich media by HPLC and accelerator mass spectrometry. Anal. Chem. 82, 9812–9817.
Taniguchi, T., Okahashi, N., Matsuda, F., 2024. ^{13}C-metabolic flux analysis reveals metabolic rewiring in HL-60 neutrophil-like cells through differentiation and immune stimulation. Metab Eng Comm 18, e00239.
Templeton, N., Smith, K.D., McAtee-Pereira, A.G., Dorai, H., Betenbaugh, M.J., Lang, S. E., Young, J.D., 2017. Application of ^{13}C flux analysis to identify high-productivity CHO metabolic phenotypes. Metab. Eng. 43, 218–225.
van Winden, W.A., Wittmann, C., Heinzle, E., Heijnen, J.J., 2002. Correcting mass isotopomer distributions for naturally occurring isotopes. Biotechnol. Bioeng. 80, 477–479.
Varahan, S., Sinha, V., Walvekar, A., Krishna, S., Laxman, S., 2020. Resource plasticity-driven carbon-nitrogen budgeting enables specialization and division of labor in a clonal community. Elife 9.
Volk, M.J., Tran, V.G., Tan, S.I., Mishra, S., Fatma, Z., Boob, A., Li, H., Xue, P., Martin, T. A., Zhao, H., 2023. Metabolic engineering: methodologies and applications. Chem. Rev. 123, 5521–5570.
Wasylenko, T.M., Stephanopoulos, G., 2015. Metabolomic and ^{13}C-metabolic flux analysis of a xylose-consuming *Saccharomyces cerevisiae* strain expressing xylose isomerase. Biotechnol. Bioeng. 112, 470–483.
Wiechert, W., 2001. ^{13}C metabolic flux analysis. Metab. Eng. 3, 195–206.
Yang, L., Venneti, S., Nagrath, D., 2017. Glutaminolysis: a hallmark of cancer metabolism. Annu. Rev. Biomed. Eng. 19, 163–194.
Yatabe, F., Okahashi, N., Seike, T., Matsuda, F., 2021. Comparative ^{13}C-metabolic flux analysis indicates elevation of ATP regeneration, carbon dioxide, and heat production in industrial *Saccharomyces cerevisiae* strains. Biotechnol. J., e2000438
Yuzawa, T., Shirai, T., Orishimo, R., Kawai, K., Kondo, A., Hirasawa, T., 2021. ^{13}C-metabolic flux analysis in glycerol-assimilating strains of *Saccharomyces cerevisiae*. J. Gen. Appl. Microbiol. 67, 142–149.
Zamboni, N., Fendt, S.M., Ruhl, M., Sauer, U., 2009. ^{13}C-based metabolic flux analysis. Nat. Protoc. 4, 878–892.
Zhang, J., van den Herik, B.M., Wahl, S.A., 2020. Alpha-ketoglutarate utilization in *Saccharomyces cerevisiae*: transport, compartmentation and catabolism. Sci. Rep. 10, 12838.